Transport and Communications Science Journal, Vol. 76, Issue 07 (09/2025), 965-979

Transport and Communications Science Journal

# VIBRATION OF FOUR-PHASE BIDIRECTIONAL FUNCTIONALLY GRADED BEAMS BASED ON TRIGONOMETRIC ENRICHED BEAM ELEMENT

**Vu Thi An Ninh**

University of Transport and Communications, No 3 Cau Giay Street, Hanoi, Vietnam

ARTICLE INFO

TYPE: Research Article
Received: 12/02/2025
Revised: 04/06/2025
Accepted: 08/09/2025
Published online: 15/09/2025
https://doi.org/10.47869/tcsj.76.7.4
* *Corresponding author*
Email: vuthianninh@utc.edu.vn

**Abstract.** Improving the convergence rate in finite element formulation plays an important role in studying the behavior of structures. This paper presents an efficient beam element to investigate the free vibration of bidirectional functionally graded beam. The beam is composed of four materials whose properties vary along both the length and thickness directions according to the power function, and these properties are evaluated by Voigt model. The equations of motion are derived using Hamilton's principle within the framework of the higher-order shear deformation beam theory. A two-node beam element is formulated by enriching the conventional Lagrange and Hermite interpolations with trigonometric functions, leading to rapid convergence. The finite element formulation has been validated through comparison with previously published results, and showing good agreement. The enriched beam element is employed to compute the natural frequencies of bidirectional functionally graded (BFG) beams under different boundary conditions. The influence of the grading indices, slenderness ratio and boundary conditions on the natural frequency is examined in detail and highlighted.

**Keywords:** BFG beam, higher-order shear deformation beam theory, free vibration, enriched beam element, finite element formula, natural frequency.



## 1. INTRODUCTION

With a high strength-to-weigh ratio, functionally graded (FG) materials – a novel type composite – are being increasingly utilized in aerospace, marine, mechanical, civil

engineering. Due to the growing application of FG materials, studying the response of FG structures is of growing importance. In recent years, numerous investigations on the vibration of FG beam using various methods have been reported. Using a new beam theory that had been developed for laminated composite beam, Sina et al. [1] analyzed the free vibration behavior of FG beam under different boundary conditions. By analytical method, their results indicated that the natural frequency predicted by new theory slightly differed from those obtained using the traditional first-order shear deformation beam theory. Wang and Li [2] employed the Levinson beam theory to analyze the free vibration behavior of FG beams, in which the influence of the material gradient parameter, the aspect ratio and the boundary conditions on the vibration response were discussed. With aid of Lagrange's equation, Kahya and Turan [3] examined both the free vibration characteristics and the buckling response of FG beams. In their work, natural frequencies and buckling loads were determined using the first-order shear deformation theory in conjunction with finite element method. Avcar and Mohammed [4] focused on analyzing the free vibration of FG beams on a Winkler-Pasternak foundation within the framework of Euler-Bernoulli beam theory. In their research, the influence of elastic foundation stiffness and material characteristics on the dimensionless frequency parameters was thoroughly examined. Katili et al. [5] employed the Unified and Integrated Timoshenko beam theory to investigate both static and free vibration problems. Previous studies focused on beams whose material properties vary continuously along the thickness direction. In subsequent reports, the researchers investigated the behavior of the beams with material properties varying along thickness and length. With the volume fraction of the constituent materials represented by an exponential function, researchers in [6–8] applied the first-order shear deformation theory to study the vibrational response of two-phase BFG beams. In Ref. [9], Vu Thi An Ninh employed different beam theories combined with the finite element method to compute the natural frequencies of BFG sandwich beams partially supported by an elastic foundation. By using the shape function as the solution of the static equations of equilibrium of an unstressed uniform Timoshenko beam, the dependence of the natural frequencies and dynamic magnification factor of four-phase BFG beam on two grading indices were examined by Nguyen et al. [10].

The finite element method plays a crucial role in analyzing structures. Improving the finite element formulation's efficiency can be achieved by increasing the number of shape functions per element without modifying the mesh. Ribeiro [11] added polynomial functions to the conventional interpolation for the axial and transverse displacements to study geometrically nonlinear vibration of the beams and phane frames. Shang et al. [12] applied the trigonometric and exponential functions to enrich the conventional finite element formulations in analyzing the dynamic elastoplastic behavior of Euler-Bernoulli beams. Hsu [13] used eriched $C^0$ element to analyze the free vibration of Timoshenko beam. In his report, a basic two-nodes linear element was enriched by both hierarchical functions and trigonometric functions. The enriched third-order shear deformation beam element proposed by Le et al. [14] proved to be efficient in evaluating free vibration and buckling responses of BFG sandwich beams. Hierarchical functions were used in their study to enrich the Lagrange and Hermite interpolations of a traditional beam element

This paper performs free vibration analysis of BFG beam using trigonometric enriched beam element. The beam consists of four different materials whose properties vary continuously along both the axial and thickness directions by a power-law distribution, and they are evaluated by Voigt model. By adopting the higher-order shear deformation beam theory for the displacement field, the beam's governing equations are derived. The natural

frequencies of the BFG beam are evaluated using a two-node beam element with the Lagrange and Hermite interpolations enriched by trigonometric functions. Numerical studies are performed to demonstrate the efficiency of enriched beam element and to examine the significant effects of grading indices, slenderness ratio, and different boundary conditions on the natural frequencies of the BFG beam.

## 2. MATHEMATICAL FORMULATION

### 2.1. Four-phase BFG beam model

Figure 1 shows a four-phase BFG beam with rectangular cross section ($b \times h$). A Cartesian coordinate system ($x$,$y$,$z$) is established with its origin at the left end of the beam, the ($x$,$y$) plane lies in the beam's mid-plane and the $z$-axis is oriented perpendicular to this plane, pointing upward.

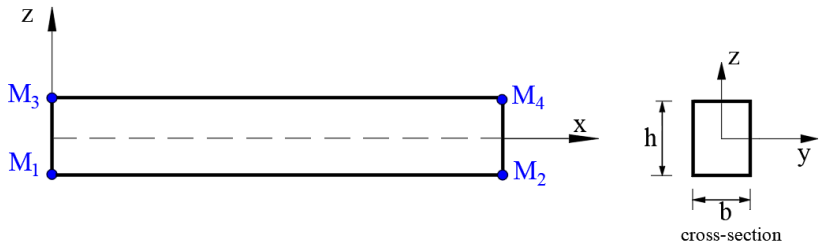


Figure 1. Geometry of four-phase BFG beam.

The beam is considered to be composed of four distinct materials, two metals ($M_1$ and $M_2$) and two ceramics ($M_3$ and $M_4$), with volume fractions that change in both the thickness and longitudinal directions as follows [10]

$$\begin{aligned} V_1 &= \left[1-\left(\frac{z}{h}+\frac{1}{2}\right)^{n_z}\right]\left[1-\left(\frac{x}{L}\right)^{n_x}\right] \\ V_2 &= \left[1-\left(\frac{z}{h}+\frac{1}{2}\right)^{n_z}\right]\left(\frac{x}{L}\right)^{n_x} \\ V_3 &= \left(\frac{z}{h}+\frac{1}{2}\right)^{n_z}\left[1-\left(\frac{x}{L}\right)^{n_x}\right] \\ V_4 &= \left(\frac{z}{h}+\frac{1}{2}\right)^{n_z}\left(\frac{x}{L}\right)^{n_x} \end{aligned} \tag{1}$$

where $V_1$, $V_2$, $V_3$ and $V_4$ represent the volume fractions of materials $M_1$, $M_2$, $M_3$ and $M_4$, respectively; $n_x$ and $n_z$ denote the grading indices in the axial and transverse directions, respectively; $L$ represents the length of the beam. According to the Voigt model, the effective properties $P_f$, namely elastic modulus $E_f$, mass density $\rho_f$, Poisson's ratio $\nu_f$ are computed as

$$P_f = P_1V_1 + P_2V_2 + P_3V_3 + P_4V_4 \tag{2}$$

with $P_i$ ($i$=1,…,4) is the property of $M_i$ ($i$=1,…,4). Combining Eqs. (1) and (2) gives us

$$P_f\left(x,z\right)=\left(P_1-P_2-P_3+P_4\right)\left(\frac{z}{h}+\frac{1}{2}\right)^{n_z}\left(\frac{x}{L}\right)^{n_x}+\left(P_2-P_1\right)\left(\frac{x}{L}\right)^{n_x}+\left(P_3-P_1\right)\left(\frac{z}{h}+\frac{1}{2}\right)^{n_z}+P_1 \tag{3}$$

If $M_1$ and $M_3$ are, respectively, identical to $M_2$ and $M_4$, then Eq. (3) simplifies to the expression for the effective properties of a two-phase transverse functionally graded beam. Furthermore, when $n_x$=0, Eq. (3) yields the effective properties of a transverse FG beam made of $M_2$ and $M_4$ [4]

$$P_f\left(z\right)=\left(P_4-P_2\right)\left(\frac{z}{h}+\frac{1}{2}\right)^{n_z}+P_2 \tag{4}$$

On the other hand, the effective properties of the axial FG beam composed of $M_3$ and $M_4$ if $n_z$=0 as

$$P_f\left(x\right)=\left(P_4-P_3\right)\left(\frac{x}{L}\right)^{n_x}+P_3 \tag{5}$$

### 2.2. Governing equations

Based on the higher - order shear deformation theory [15], the displacements of a point in the $x$ and $z$ direction are, respectively, given by

$$\begin{aligned} u_1\left(x,z,t\right)&=u\left(x,t\right)-zw_{b,x}\left(x,t\right)+f\left(z\right)w_{s,x}\left(x,t\right)\\ u_3\left(x,z,t\right)&=w_b\left(x,t\right)+w_s\left(x,t\right)\end{aligned} \tag{6}$$

In Eq. (6), $u(x,t)$ represents the axial displacement at a point along the $x$-axis; $w_b(x,t)$ and $w_s(x,t)$ denote the bending and shear components of transverse displacement, respectively; $t$ represents the time variable; in the above equation and in what follows, a subscript comma indicates the derivative with respect to the variable that follows, and

$$f\left(z\right)=-\frac{4z^3}{3h^2} \tag{7}$$

From Eq. (6), the axial strain $\varepsilon_{xx}$ and shear strain $\gamma_{xz}$ can be expressed as follows

$$\varepsilon_{xx}=u_{,x}-zw_{b,xx}+f\left(z\right)w_{s,xx},\quad \gamma_{xz}=\left(1+f_{,z}\right)w_{s,x} \tag{8}$$

The axial and shear stressess, $\sigma_{xx}$ and $\tau_{xz}$, have the following form

$$\sigma_{xx}=E_f\left(x,z\right)\varepsilon_{xx},\quad \tau_{xz}=G_f\left(x,z\right)\gamma_{xz} \tag{9}$$

where $G_f\left(x,z\right)=\dfrac{E_f\left(x,z\right)}{2\left[1+\nu_f\left(x,z\right)\right]}$ is the effective shear modulus.

The elastic strain energy of the beam $U$ is given by

$$U = \frac{1}{2}\int_0^L \int_A \left(\sigma_{xx}\varepsilon_{xx} + \tau_{xz}\gamma_{xz}\right) dAdx \tag{10}$$

Here, $A=bh$ denotes the beam's cross-section area. From Eqs. (8), (9) and (10), the expression for the strain energy of the beam can be reformulated as follows

$$\begin{aligned} U = \frac{1}{2}\int_0^L \Big[ & A_{11}u_{,x}^2 - 2A_{12}u_{,x}w_{b,xx} + A_{22}w_{b,xx}^2 + 2A_{13}u_{,x}w_{s,xx} \\ & -2A_{23}w_{b,xx}w_{s,xx} + A_{33}w_{\mathrm{s},xx}^2 + B_{33}w_{s,x}^2 \Big] dx \end{aligned} \tag{11}$$

where the beam rigidities $A_{11}, A_{12}, A_{22}, A_{13}, A_{23}, A_{33}$ and $B_{33}$ are expressed by

$$\begin{aligned} \left(A_{11}, A_{12}, A_{22}, A_{13}, A_{23}, A_{33}\right) &= \int_A E_f\left(x,z\right)\left[1, \mathrm{z}, \mathrm{z}^2, f\left(z\right), \mathrm{z}\, f\left(z\right), f^2\left(z\right)\right] dA \\ B_{33} &= \int_A G_f\left(x,z\right)\left(1 + f_{,z}\right)^2 dA \end{aligned} \tag{12}$$

The beam's kinetic energy $T$ is defined by

$$T = \frac{1}{2}\int_0^L \int_A \rho_f\left(x,z\right)\left(\dot{u}_1^2 + \dot{u}_3^2\right) dAdx \tag{13}$$

in above equation and hereafter, an over dot denotes the derivative with respect to the time variable. Eq. (6) allows the kinetic energy $T$ in Eq. (13) to be expressed in the following form

$$T = \frac{1}{2}\int_0^L \left\{ I_{11}\left[\dot{u}^2 + \left(\dot{w}_b + \dot{w}_s\right)^2\right] - 2I_{12}\dot{u}\dot{w}_{b,x} + I_{22}\dot{w}_{b,x}^2 + 2I_{13}\dot{u}\dot{w}_{\mathrm{s},x} - 2I_{23}\dot{w}_{\mathrm{b},x}\dot{w}_{\mathrm{s},x} + I_{33}\dot{w}_{\mathrm{s},x}^2 \right\} dx \tag{14}$$

where $I_{11}, I_{12}, I_{22}, I_{13}, I_{23}, I_{33}$ are the mass moments and it is defined by

$$\left(I_{11}, I_{12}, I_{22}, I_{13}, I_{23}, I_{33}\right) = \int_A \rho_f\left(x,z\right)\left[1, z, z^2, f\left(z\right), zf\left(z\right), f^2\left(z\right)\right] dA \tag{15}$$

Hamilton's principle applied to Eqs. (11) and (14) yields the differential equations of motion for the beam as below

$$\begin{aligned} \delta u &: -\left(I_{11}\ddot{u} - I_{12}\ddot{w}_{b,x} + I_{13}\ddot{w}_{s,x}\right) + \left(A_{11}u_{,x} - A_{12}w_{b,xx} + A_{13}w_{s,xx}\right)_{,x} = 0 \\ \delta w_b &: -I_{11}\left(\ddot{w}_b + \ddot{w}_s\right) + \left(-I_{12}\ddot{u} + I_{22}\ddot{w}_{b,x} - I_{23}\ddot{w}_{s,x}\right)_{,x} - \left(A_{12}u_{,x} + A_{22}w_{b,xx} - A_{23}w_{s,xx}\right)_{,xx} = 0 \\ \delta w_s &: -I_{11}\left(\ddot{w}_b + \ddot{w}_s\right) + \left(I_{13}\ddot{u} - I_{23}\ddot{w}_{b,x} + I_{33}\ddot{w}_{s,x}\right)_{,x} \\ & \quad -\left(A_{13}u_{,x} - A_{23}w_{b,xx} + A_{33}w_{s,xx}\right)_{,xx} + \left(B_{33}w_{s,x}\right)_{,x} = 0 \end{aligned} \tag{16}$$

## 3. FINITE ELEMENT FORMULATION

### 3.1. Enriched beam element

Assume a conventional two-node beam element having length $l$, the element's nodal displacement vector consisting of ten degrees of freedom is represented as follows

$$\underset{(10\times1)}{\hat{\mathbf{d}}} = \left\{\mathbf{d}_u \quad \mathbf{d}_{w_b} \quad \mathbf{d}_{w_s}\right\}^T \tag{17}$$

where

$$\mathbf{d}_u = \left\{u_1 \quad u_2\right\}^T, \quad \mathbf{d}_{w_b} = \left\{w_{b1} \quad w_{bx1} \quad w_{b2} \quad w_{bx2}\right\}^T, \quad \mathbf{d}_{w_s} = \left\{w_{s1} \quad w_{sx1} \quad w_{s2} \quad w_{sx2}\right\}^T \tag{18}$$

are the nodal displacement vectors for $u, w_b$ and $w_s$ at nodes 1 and 2. The displacements are interpolated from these nodal displacements as follows

$$u = \mathbf{N}\mathbf{d}_u, \quad w_b = \mathbf{H}\mathbf{d}_{w_b}, \quad w_s = \mathbf{H}\mathbf{d}_{w_s} \tag{19}$$

here $\mathbf{N} = \begin{bmatrix} N_1 & N_2 \end{bmatrix}$, $\mathbf{H} = \begin{bmatrix} H_1 & H_2 & H_3 & H_4 \end{bmatrix}$ are the matrices of the following Lagrange and Hermite shape function.

$$N_1 = \frac{l-x}{l}, \quad N_2 = \frac{x}{l} \tag{20}$$

and

$$H_1 = 1-3\frac{x^2}{l^2}+2\frac{x^3}{l^3}, \quad H_2 = x-2\frac{x^2}{l}+\frac{x^3}{l^2}, \quad H_3 = 3\frac{x^2}{l^2}-2\frac{x^3}{l^3}, \quad H_4 = -\frac{x^2}{l}+\frac{x^3}{l^2} \tag{21}$$

By substituting Eqs. (17)-(21) into Eqs. (11) and (14), the stiffness and mass matrices for analyzing the free vibration of bidirectional four-phase FG beam can be obtained.

In order to improve the beam element's efficiency, the Lagrange and Hermite interpolation described above are enriched by trigonometric functions. Here, four trigonometric functions are used to supplement the original interpolation functions, the displacements in Eq. (19) are rewritten as

$$u = \mathbf{N}\mathbf{d}_u + \mathbf{N}^*\mathbf{d}_u^*, \quad w_b = \mathbf{H}\mathbf{d}_{w_b} + \mathbf{H}^*\mathbf{d}_{w_b}^*, \quad w_s = \mathbf{H}\mathbf{d}_{w_s} + \mathbf{H}^*\mathbf{d}_{w_s}^* \tag{22}$$

where $\mathbf{N}^* = \begin{bmatrix} N_3 & N_4 & N_5 & N_6 \end{bmatrix}$ and $\mathbf{H}^* = \begin{bmatrix} H_5 & H_6 & H_7 & H_8 \end{bmatrix}$ represent the enriched shape function matrices; the vectors $\mathbf{d}_u^*, \mathbf{d}_{w_b}^*, \mathbf{d}_{w_s}^*$ are the supplemented unknowns, defined as follows

$$\mathbf{d}_u^* = \left\{a_1 \quad a_2 \quad a_3 \quad a_4\right\}^T, \quad \mathbf{d}_{w_b}^* = \left\{b_1 \quad b_2 \quad b_3 \quad b_4\right\}^T, \quad \mathbf{d}_{w_s}^* = \left\{s_1 \quad s_2 \quad s_3 \quad s_4\right\}^T \tag{23}$$

The trigonometric functions are used to define the functions $N_i$ ($i$=3…6) and $H_j$ ($j$=5…8) as follows [11]

$$\begin{aligned} N_3 &= N_1\left[\cos\left(\frac{\pi x}{l}\right)-1\right], \quad N_4 = N_1\left[\cos\left(\frac{2\pi x}{l}\right)-1\right], \\ N_5 &= N_2\left[\cos\pi\left(1-\frac{x}{l}\right)-1\right], \quad N_6 = N_2\left[\cos 2\pi\left(1-\frac{x}{l}\right)-1\right] \end{aligned} \tag{24}$$

and

$$H_5 = H_1\left[\cos\left(\frac{\pi x}{l}\right)-1\right], \quad H_6 = H_2\left[\cos\left(\frac{\pi x}{l}\right)-1\right],$$
$$H_7 = H_3\left[\cos\pi\left(1-\frac{x}{l}\right)-1\right], \quad H_8 = H_4\left[\cos\pi\left(1-\frac{x}{l}\right)-1\right] \tag{25}$$

Using the enriched interpolations, the degrees of freedom vector **d** for an element consisting of 22 components is expressed as follows

$$\underset{(22\times1)}{\mathbf{d}} = \left\{\mathbf{d}_u \quad \mathbf{d}_u^* \quad \mathbf{d}_{w_b} \quad \mathbf{d}_{w_b}^* \quad \mathbf{d}_{w_s} \quad \mathbf{d}_{w_s}^*\right\}^T \tag{26}$$

### 3.2. Element stiffness and mass matrices

Based on the above enrichment interpolation, the expression for the beam's strain energy in Eq. (11) is reformulated as follows

$$U = \frac{1}{2}\sum_{i=1}^{nel}\mathbf{d}_i^T\mathbf{k}_i\mathbf{d}_i \tag{27}$$

here *nel* refers to the total number of discretized beam elements; $\mathbf{k}_i$ represents the stiffness matrix of the beam element and it is defined in the form of sub-matrix below

$$\mathbf{k}_i = \begin{bmatrix}
\mathbf{k}_{uu} & \mathbf{k}_{uu^*} & \mathbf{k}_{uw_b} & \mathbf{k}_{uw_b^*} & \mathbf{k}_{uw_s} & \mathbf{k}_{uw_s^*} \\
\left(\mathbf{k}_{uu^*}\right)^T & \mathbf{k}_{u^*u^*} & \mathbf{k}_{u^*w_b} & \mathbf{k}_{u^*w_b^*} & \mathbf{k}_{u^*w_s} & \mathbf{k}_{u^*w_s^*} \\
\left(\mathbf{k}_{uw_b}\right)^T & \left(\mathbf{k}_{u^*w_b}\right)^T & \mathbf{k}_{w_bw_b} & \mathbf{k}_{w_bw_b^*} & \mathbf{k}_{w_bw_s} & \mathbf{k}_{w_bw_s^*} \\
\left(\mathbf{k}_{uw_b^*}\right)^T & \left(\mathbf{k}_{u^*w_b^*}\right)^T & \left(\mathbf{k}_{w_bw_b^*}\right)^T & \mathbf{k}_{w_b^*w_b^*} & \mathbf{k}_{w_b^*w_s} & \mathbf{k}_{w_b^*w_s^*} \\
\left(\mathbf{k}_{uw_s}\right)^T & \left(\mathbf{k}_{u^*w_s}\right)^T & \left(\mathbf{k}_{w_bw_s}\right)^T & \left(\mathbf{k}_{w_b^*w_s}\right)^T & \mathbf{k}_{w_sw_s} & \mathbf{k}_{w_sw_s^*} \\
\left(\mathbf{k}_{uw_s^*}\right)^T & \left(\mathbf{k}_{u^*w_s^*}\right)^T & \left(\mathbf{k}_{w_bw_s^*}\right)^T & \left(\mathbf{k}_{w_b^*w_s^*}\right)^T & \left(\mathbf{k}_{w_sw_s^*}\right)^T & \mathbf{k}_{w_s^*w_s^*}
\end{bmatrix} \tag{28}$$

The sub-matrices in Eq. (28) are determined

$$\underset{(2\times2)}{\mathbf{k}_{uu}} = \int_0^l \mathbf{N}_{,x}^T A_{11}\mathbf{N}_{,x}dx, \quad \underset{(2\times4)}{\mathbf{k}_{uu^*}} = \int_0^l \mathbf{N}_{,x}^T A_{11}\mathbf{N}_{,x}^*dx, \quad \underset{(2\times4)}{\mathbf{k}_{uw_b}} = -\int_0^l \mathbf{N}_{,x}^T A_{12}\mathbf{H}_{,xx}dx,$$
$$\underset{(2\times4)}{\mathbf{k}_{uw_b^*}} = -\int_0^l \mathbf{N}_{,x}^T A_{12}\mathbf{H}_{,xx}^*dx, \quad \underset{(2\times4)}{\mathbf{k}_{uw_s}} = \int_0^l \mathbf{N}_{,x}^T A_{13}\mathbf{H}_{,xx}dx, \quad \underset{(2\times4)}{\mathbf{k}_{uw_s^*}} = \int_0^l \mathbf{N}_{,x}^T A_{13}\mathbf{H}_{,xx}^*dx,$$

$$
\begin{aligned}
&\underset{(4\times4)}{\mathbf{k}_{u^*u^*}} = \int_0^l \mathbf{N}_{,x}^{*T} A_{11} \mathbf{N}_{,x}^{*} dx, \quad \underset{(4\times4)}{\mathbf{k}_{u^*w_b}} = -\int_0^l \mathbf{N}_{,x}^{*T} A_{12} \mathbf{H}_{,xx} dx, \quad \underset{(4\times4)}{\mathbf{k}_{u^*w_b^*}} = -\int_0^l \mathbf{N}_{,x}^{*T} A_{12} \mathbf{H}_{,xx}^{*} dx, \\
&\underset{(4\times4)}{\mathbf{k}_{u^*w_s}} = \int_0^l \mathbf{N}_{,x}^{*T} A_{13} \mathbf{H}_{,xx} dx, \quad \underset{(4\times4)}{\mathbf{k}_{u^*w_s^*}} = \int_0^l \mathbf{N}_{,x}^{*T} A_{13} \mathbf{H}_{,xx}^{*} dx, \quad \underset{(4\times4)}{\mathbf{k}_{w_b w_b}} = \int_0^l \mathbf{H}_{,xx}^{T} A_{22} \mathbf{H}_{,xx} dx, \\
&\underset{(4\times4)}{\mathbf{k}_{w_b w_b^*}} = \int_0^l \mathbf{H}_{,xx}^{T} A_{22} \mathbf{H}_{,xx}^{*} dx, \quad \underset{(4\times4)}{\mathbf{k}_{w_b w_s}} = -\int_0^l \mathbf{H}_{,xx}^{T} A_{23} \mathbf{H}_{,xx} dx, \quad \underset{(4\times4)}{\mathbf{k}_{w_b w_s^*}} = -\int_0^l \mathbf{H}_{,xx}^{T} A_{23} \mathbf{H}_{,xx}^{*} dx, \\
&\underset{(4\times4)}{\mathbf{k}_{w_b^* w_b^*}} = \int_0^l \mathbf{H}_{,xx}^{*T} A_{22} \mathbf{H}_{,xx}^{*} dx, \quad \underset{(4\times4)}{\mathbf{k}_{w_b^* w_s}} = -\int_0^l \mathbf{H}_{,xx}^{*T} A_{23} \mathbf{H}_{,xx} dx, \quad \underset{(4\times4)}{\mathbf{k}_{w_b^* w_s^*}} = -\int_0^l \mathbf{H}_{,xx}^{*T} A_{23} \mathbf{H}_{,xx}^{*} dx, \\
&\underset{(4\times4)}{\mathbf{k}_{w_s w_s}} = \int_0^l \left( \mathbf{H}_{,xx}^{T} A_{33} \mathbf{H}_{,xx} + \mathbf{H}_{,x}^{T} B_{33} \mathbf{H}_{,x} \right) dx, \quad \underset{(4\times4)}{\mathbf{k}_{w_s w_s^*}} = \int_0^l \left( \mathbf{H}_{,xx}^{T} A_{33} \mathbf{H}_{,xx}^{*} + \mathbf{H}_{,x}^{T} B_{33} \mathbf{H}_{,x}^{*} \right) dx, \\
&\underset{(4\times4)}{\mathbf{k}_{w_s^* w_s^*}} = \int_0^l \left( \mathbf{H}_{,xx}^{*T} A_{33} \mathbf{H}_{,xx}^{*} + \mathbf{H}_{,x}^{*T} B_{33} \mathbf{H}_{,x}^{*} \right) dx
\end{aligned}
\tag{29}
$$

Eq. (14) for the kinetic energy can also be expressed as

$$
T = \frac{1}{2} \sum_{i=1}^{nel} \dot{\mathbf{d}}_i^T \, \mathbf{m}_i \dot{\mathbf{d}}_i \tag{30}
$$

where $\mathbf{m}_i$ is the element mass matrix and it is defined as

$$
\mathbf{m}_i = \begin{bmatrix}
\mathbf{m}_{uu} & \mathbf{m}_{uu^*} & \mathbf{m}_{uw_b} & \mathbf{m}_{uw_b^*} & \mathbf{m}_{uw_s} & \mathbf{m}_{uw_s^*} \\
\left(\mathbf{m}_{uu^*}\right)^T & \mathbf{m}_{u^*u^*} & \mathbf{m}_{u^*w_b} & \mathbf{m}_{u^*w_b^*} & \mathbf{m}_{u^*w_s} & \mathbf{m}_{u^*w_s^*} \\
\left(\mathbf{m}_{uw_b}\right)^T & \left(\mathbf{m}_{u^*w_b}\right)^T & \mathbf{m}_{w_b w_b} & \mathbf{m}_{w_b w_b^*} & \mathbf{m}_{w_b w_s} & \mathbf{m}_{w_b w_s^*} \\
\left(\mathbf{m}_{uw_b^*}\right)^T & \left(\mathbf{m}_{u^*w_b^*}\right)^T & \left(\mathbf{m}_{w_b w_b^*}\right)^T & \mathbf{m}_{w_b^* w_b^*} & \mathbf{m}_{w_b^* w_s} & \mathbf{m}_{w_b^* w_s^*} \\
\left(\mathbf{m}_{uw_s}\right)^T & \left(\mathbf{m}_{u^*w_s}\right)^T & \left(\mathbf{m}_{w_b w_s}\right)^T & \left(\mathbf{m}_{w_b^* w_s}\right)^T & \mathbf{m}_{w_s w_s} & \mathbf{m}_{w_s w_s^*} \\
\left(\mathbf{m}_{uw_s^*}\right)^T & \left(\mathbf{m}_{u^*w_s^*}\right)^T & \left(\mathbf{m}_{w_b w_s^*}\right)^T & \left(\mathbf{m}_{w_b^* w_s^*}\right)^T & \left(\mathbf{m}_{w_s w_s^*}\right)^T & \mathbf{m}_{w_s^* w_s^*}
\end{bmatrix}
\tag{31}
$$

The components in matrix $\mathbf{m}_i$ are defined as

$$
\begin{aligned}
&\underset{(2\times2)}{\mathbf{m}_{uu}} = \int_0^l \mathbf{N}^T I_{11} \mathbf{N} dx, \quad \underset{(2\times4)}{\mathbf{m}_{uu^*}} = \int_0^l \mathbf{N}^T I_{11} \mathbf{N}^{*} dx, \quad \underset{(2\times4)}{\mathbf{m}_{uw_b}} = -\int_0^l \mathbf{N}^T I_{12} \mathbf{H}_{,\mathrm{x}} dx, \\
&\underset{(2\times4)}{\mathbf{m}_{uw_b^*}} = -\int_0^l \mathbf{N}^T I_{12} \mathbf{H}_{,\mathrm{x}}^{*} dx, \quad \underset{(2\times4)}{\mathbf{m}_{uw_s}} = \int_0^l \mathbf{N}^T I_{13} \mathbf{H}_{,\mathrm{x}} dx, \quad \underset{(2\times4)}{\mathbf{m}_{uw_s^*}} = \int_0^l \mathbf{N}^T I_{13} \mathbf{H}_{,x}^{*} dx, \\
&\underset{(4\times4)}{\mathbf{m}_{u^*u^*}} = \int_0^l \mathbf{N}^{*T} I_{11} \mathbf{N}^{*} dx, \quad \underset{(4\times4)}{\mathbf{m}_{u^*w_b}} = -\int_0^l \mathbf{N}^{*T} I_{12} \mathbf{H}_{,x} dx, \quad \underset{(4\times4)}{\mathbf{m}_{u^*w_b^*}} = -\int_0^l \mathbf{N}^{*T} I_{12} \mathbf{H}_{,x}^{*} dx,
\end{aligned}
$$

$$\underset{(4\times4)}{\mathbf{m}_{u^*w_s}}=\int_0^l \mathbf{N}^{*T}I_{13}\mathbf{H}_{,x}dx,\quad \underset{(4\times4)}{\mathbf{m}_{u^*w_s^*}}=\int_0^l \mathbf{N}^{*T}I_{13}\mathbf{H}^*_{,x}dx,\quad \underset{(4\times4)}{\mathbf{m}_{w_bw_b}}=\int_0^l \left(\mathbf{H}^TI_{11}\mathbf{H}+\mathbf{H}^T_{,x}I_{22}\mathbf{H}_{,x}\right)dx,$$

$$\underset{(4\times4)}{\mathbf{m}_{w_bw_b^*}}=\int_0^l \left(\mathbf{H}^TI_{11}\mathbf{H}^*+\mathbf{H}^T_{,x}I_{22}\mathbf{H}^*_{,x}\right)dx,\quad \underset{(4\times4)}{\mathbf{m}_{w_bw_s}}=-\int_0^l \mathbf{H}^T_{,x}I_{23}\mathbf{H}_{,x}dx,\quad \underset{(4\times4)}{\mathbf{m}_{w_bw_s^*}}=-\int_0^l \mathbf{H}^T_{,x}I_{23}\mathbf{H}^*_{,x}dx,$$

$$\underset{(4\times4)}{\mathbf{m}_{w_b^*w_b^*}}=\int_0^l \left(\mathbf{H}^{*T}I_{11}\mathbf{H}^*+\mathbf{H}^{*T}_{,x}I_{22}\mathbf{H}^*_{,x}\right)dx,\quad \underset{(4\times4)}{\mathbf{m}_{w_b^*w_s}}=-\int_0^l \mathbf{H}^{*T}_{,x}I_{23}\mathbf{H}_{,x}dx,\quad \underset{(4\times4)}{\mathbf{m}_{w_b^*w_s^*}}=-\int_0^l \mathbf{H}^{*T}_{,x}I_{23}\mathbf{H}^*_{,x}dx, \tag{32}$$

$$\underset{(4\times4)}{\mathbf{m}_{w_sw_s}}=\int_0^l \left(\mathbf{H}^TI_{11}\mathbf{H}+\mathbf{H}^T_{,x}I_{33}\mathbf{H}_{,x}\right)dx,\quad \underset{(4\times4)}{\mathbf{m}_{w_sw_s^*}}=\int_0^l \left(\mathbf{H}^TI_{11}\mathbf{H}^*+\mathbf{H}^T_{,x}I_{33}\mathbf{H}^*_{,x}\right)dx,$$

$$\underset{(4\times4)}{\mathbf{m}_{w_s^*w_s^*}}=\int_0^l \left(\mathbf{H}^{*T}I_{11}\mathbf{H}^*+\mathbf{H}^{*T}_{,x}I_{33}\mathbf{H}^*_{,x}\right)dx$$

### 3.3. Discrete equation of motion

Using the derived element stiffness and mass matrices, the equations of motion for BFG beam can be expressed as follows

$$\mathbf{M}\ddot{\mathbf{D}}+\mathbf{K}\mathbf{D}=\mathbf{0} \tag{33}$$

where $\mathbf{D}$, $\ddot{\mathbf{D}}$ denote the nodal displacement and acceleration vectors; $\mathbf{M}$ and $\mathbf{K}$ represent the global mass and stiffness matrices, respectivey, assembled from the element matrices $\mathbf{m}_i$ and $\mathbf{k}_i$. By representing the nodal displacement vector as a harmonic function in free vibration analysis, Eq. (33) yields an eigenvalue problem for computing the natural frequency $\omega$ as follows

$$\left(\mathbf{K}-\omega^2\mathbf{M}\right)\bar{\mathbf{D}}=\mathbf{0} \tag{34}$$

where $\bar{\mathbf{D}}$ represents the vibration amplitude. A standard method, as provided in [16], can be employed to solve Eq. (34).

## 4. NUMERICAL ANALYSIS AND DISCUSSION

A numerical investigation is performed in this section to confirm the effectiveness of the enriched beam element and to analyze the effects of the geometrical and material properties on the BFG beam's free vibration. The beam used in the analysis has dimendions $h$=1 m, $b$=0.5 m and is considered under three distinct boundary conditions:

- For simply-supported (S-S) beam: $u(0,t)=w_b(0,t)=w_s(0,t)=w_b(L,t)=w_s(L,t)=0$
- For clamped-clamped (C-C) beam: $u(0,t)=w_b(0,t)=w_s(0,t)=w_{b,x}(0,t)=w_{s,x}(0,t)=0$ and $u(L,t)=w_b(L,t)=w_s(L,t)=w_{b,x}(L,t)=w_{s,x}(L,t)=0$
- For clamped-free (C-F) beam: $u(0,t)=w_b(0,t)=w_s(0,t)=w_{b,x}(0,t)=w_{s,x}(0,t)=0$

In this study, the BFG beam consists of four constituent materials: stainless steel (SUS304) as $M_1$, aluminum (Al) as $M_2$, alumina ($Al_2O_3$) as $M_3$ and zirconia ($ZrO_2$) as $M_4$. The properties of these materials are as follows [10]

- $E_1$=210 GPa, $\rho_1$=7800 kg/m$^3$, $\nu_1$=0.3 for steel
- $E_2$=70 GPa, $\rho_2$=2702 kg/m$^3$, $\nu_2$=0.23 for aluminum
- $E_3$=390 GPa, $\rho_3$=3960 kg/m$^3$, $\nu_3$=0.3 for alumina
- $E_4$=200 GPa, $\rho_4$=5700 kg/m$^3$, $\nu_4$=0.3 for zirconia

The frequency parameter is defined as

$$\mu_i = \omega_i \frac{L^2}{h}\sqrt{\frac{\rho_2}{E_2}} \tag{35}$$

where $\omega_i$ is the $i$th natural frequency.

The proposed beam element's accuracy in this study is verified by comparison with previous work. Firstly, in the table 1, the fundamental frequency parameters for the two-phase FG beam under S-S, C-C, C-F boundary conditions are calculated and compared with those obtained by Avcar and Mohammed [4] using Euler-Bernoulli beam theory. In this table, the beam made of Al and $Al_2O_3$, and their material properties vary along the thickness direction. As seen from table 1, the results obtained in this study show good agreement with those reported in Ref. [4], irrespective of the index $n_z$ and boundary conditions.

Table 1. Comparison of the fundamental frequency parameter for a two-phase FG beam under different boundary conditions ($n_x$=0, $L/h$=20).

| BC | Source | $Al_2O_3$ | $n_z$=1 | $n_z$=2 | $n_z$=10 | Al |
|---|---|---|---|---|---|---|
| SS | Ref. [4] | 5.483 | 4.221 | 3.852 | 3.559 | 2.849 |
| | Present | 5.460 | 4.204 | 3.834 | 3.538 | 2.837 |
| CC | Ref. [4] | 12.43 | 9.569 | 8.732 | 8.068 | 6.459 |
| | Present | 12.222 | 9.431 | 8.597 | 7.885 | 6.351 |
| CF | Ref. [4] | 1.953 | 1.504 | 1.372 | 1.268 | 1.015 |
| | Present | 1.950 | 1.501 | 1.370 | 1.265 | 1.013 |

To further verify the accuracy of the above formulas, the frequency parameter $\mu_1$ of the S-S bidirectional FG beam composed of four materials are computed and compared with that obtained by Timoshenko beam theory in Ref. [10], as shown in table 2. Regardless of axial and transverse grading indices, table 2 demonstrates good agreement between the results of the present study and those reported in Ref. [10].

Table 2. Comparison of the frequency parameter $\mu_1$ of the S-S bidirectional four-phase FG beam ($L/h$=20).

| $n_z$ | Source | $n_x$=0 | $n_x$=1/3 | $n_x$=1/2 | $n_x$=5/6 | $n_x$=1 | $n_x$=4/3 | $n_x$=3/2 | $n_x$=2 |
|---|---|---|---|---|---|---|---|---|---|
| 0 | Ref. [10] | 3.3018 | 3.7429 | 3.9148 | 4.1968 | 4.3139 | 4.5118 | 4.5956 | 4.8005 |
| | Present | 3.3018 | 3.7430 | 3.9149 | 4.1971 | 4.3142 | 4.5121 | 4.5960 | 4.8008 |
| 1/3 | Ref. [10] | 3.1542 | 3.5050 | 3.6305 | 3.8252 | 3.9022 | 4.0277 | 4.0792 | 4.2009 |
| | Present | 3.1827 | 3.5302 | 3.6549 | 3.8484 | 3.9250 | 4.0498 | 4.1010 | 4.2221 |

| | | | | | | | | | |
|---|---|---|---|---|---|---|---|---|---|
| 1/2 | Ref. [10] | 3.1068 | 3.4285 | 3.5397 | 3.7087 | 3.7745 | 3.8805 | 3.9236 | 4.0245 |
| | Present | 3.1560 | 3.4708 | 3.5801 | 3.7465 | 3.8113 | 3.9158 | 3.9582 | 4.0578 |
| 5/6 | Ref. [10] | 3.0504 | 3.3296 | 3.4206 | 3.5548 | 3.6059 | 3.6869 | 3.7194 | 3.7947 |
| | Present | 3.1361 | 3.4003 | 3.4871 | 3.6156 | 3.6646 | 3.7425 | 3.7737 | 3.8462 |
| 1 | Ref. [10] | 3.0359 | 3.2984 | 3.3819 | 3.5035 | 3.5495 | 3.6219 | 3.6508 | 3.7177 |
| | Present | 3.1355 | 3.3792 | 3.4575 | 3.5721 | 3.6155 | 3.6841 | 3.7116 | 3.7750 |

Table 3 demonstrates the efficiency of the proposed beam element through the evaluation of the fundamental frequency parameters of S-S BFG beam. Both the enriched beam element (EBE) and conventional beam element (CBE) are calculated with different values of the grading indices. As obverved in table 3, EBE converges very fast, it only needs 2 elements while CBE requires 20 elements to converge, regardless of the grading indices. Thus, element enrichment significantly improves the efficiency of the beam element in evaluating the frequency parameter of four-phase BFG beam.

Table 3. Convergence study of the beam elements for calculating the fundamental frequency parameter of the S-S bidirectional four-phase FG beam (L/h=10).

| $n_x$ | $n_z$ | Element type | *nel*=1 | *nel*=2 | *nel*=4 | *nel*=6 | *nel*=16 | *nel*=18 | *nel*=20 |
|---|---|---|---|---|---|---|---|---|---|
| 0.3 | 0.5 | EBE | 3.4068 | 3.4068 | 3.4068 | -* | - | - | - |
| | | CBE | 3.8022 | 3.4303 | 3.4102 | 3.4081 | 3.4069 | 3.4068 | 3.4068 |
| | 3 | EBE | 3.2478 | 3.2478 | 3.2478 | - | - | - | - |
| | | CBE | 3.6374 | 3.2826 | 3.2545 | 3.2505 | 3.2481 | 3.2478 | 3.2478 |
| 1 | 0.5 | EBE | 3.7657 | 3.7657 | 3.7657 | - | - | - | - |
| | | CBE | 4.1225 | 3.7933 | 3.7695 | 3.7671 | 3.7659 | 3.7657 | 3.7657 |
| | 3 | EBE | 3.3357 | 3.3356 | 3.3356 | - | - | - | - |
| | | CBE | 3.6531 | 3.3679 | 3.3419 | 3.3383 | 3.3360 | 3.3359 | 3.3356 |

Note: * unchanged

The frequency parameter $\mu_1$ of the BFG beam with boundary conditions S-S, C-C, C-F is shown in table 4. The results in the beam are calculated with different values of $n_x$, $n_z$ and $L/h$. The table clearly shows that the parameter $\mu_1$ depends significantly on the grading indices, an increase in the axial grading index $n_x$ leads to a rise in the parameter $\mu_1$, whereas an increase in the transverse grading index $n_z$ results in its reduction. The influence of the grading indices on the frequency parameter can be understood through the variation in material composition resulting from changes in $n_x$ and $n_z$. As seen from Eq. (1), the beam with higher $n_x$ has higher percentage of $M_1$ and $M_3$, lower percentage of $M_2$ and $M_4$. Under the materials used in this study, the stiffness of the beam increases, thereby causing a rise in the frequency parameter. A similar explanation for the reduction in the frequency parameter with increasing index $n_z$. The table 4 also shows that the beam with $L/h$=5 exhibits a smaller frequency parameter $\mu_1$ than the beam with $L/h$=20, regardless of the values of the grading indices or the boundary conditions. Furthermore, the C-C beam yieds the highest frequency parameter, while the C-F beam results the lowest frequency parameter value.

Table 4. Frequency parameter $\mu_1$ of the four-phase BFG beam.

| | | *L*/*h*=5 | | | | *L*/*h*=20 | | | |
|---|---|---|---|---|---|---|---|---|---|
| BC | $n_x$ | $n_z$=0.5 | $n_z$=1 | $n_z$=2 | $n_z$=5 | $n_z$=0.5 | $n_z$=1 | $n_z$=2 | $n_z$=5 |
| SS | 0.3 | 3.2647 | 3.1808 | 3.1239 | 3.0489 | 3.4461 | 3.3611 | 3.3125 | 3.2473 |
| | 1 | 3.6015 | 3.4135 | 3.2544 | 3.0816 | 3.8113 | 3.6155 | 3.4573 | 3.2858 |
| | 3 | 3.9318 | 3.6203 | 3.3607 | 3.1091 | 4.1787 | 3.8507 | 3.5853 | 3.3292 |
| | 5 | 4.0282 | 3.6786 | 3.3917 | 3.1209 | 4.2842 | 3.9156 | 3.6209 | 3.3442 |
| CC | 0.3 | 6.4852 | 6.2613 | 6.0777 | 5.9148 | 7.7936 | 7.5268 | 7.3786 | 7.3132 |
| | 1 | 6.9773 | 6.5523 | 6.1774 | 5.8262 | 8.3924 | 7.8853 | 7.4988 | 7.1769 |
| | 3 | 7.3222 | 6.6649 | 6.1091 | 5.6144 | 8.8248 | 8.0371 | 7.4253 | 6.9116 |
| | 5 | 7.4479 | 6.7221 | 6.1198 | 5.5928 | 8.9723 | 8.1034 | 7.4344 | 6.8770 |
| CF | 0.3 | 1.3116 | 1.2969 | 1.3031 | 1.3242 | 1.3502 | 1.3359 | 1.3455 | 1.3724 |
| | 1 | 1.4800 | 1.4527 | 1.4427 | 1.4402 | 1.5247 | 1.4982 | 1.4917 | 1.4941 |
| | 3 | 1.5420 | 1.4759 | 1.4262 | 1.3814 | 1.5872 | 1.5211 | 1.4731 | 1.4307 |
| | 5 | 1.5403 | 1.4533 | 1.3849 | 1.3233 | 1.5848 | 1.4971 | 1.4295 | 1.3691 |

Figure 2 shows the variation of the first four frequency parameters with respect to the grading indices for beams with S-S, C-C, and C-F boundary conditions. In the figure, the resuts are shown for the case of a beam with *L*/*h*=20. According to the figure, the higher frequency parameter exhibit a similar dependence on the grading indices as the fundamental frequency parameter. Irrespective of the applied boundary conditions, increasing $n_x$ results in higher frequency parameters, while increasing $n_z$ causes them to decrease. The effect of the grading indices on the frequency parameters is attributed to variations in the proportions of constituent material, as discussed in table 4. Figure 2 demonstrates that the desired frequency parameters of the four-phase BFG beam can be achieved through suitable selection of $n_x$ and $n_z$.

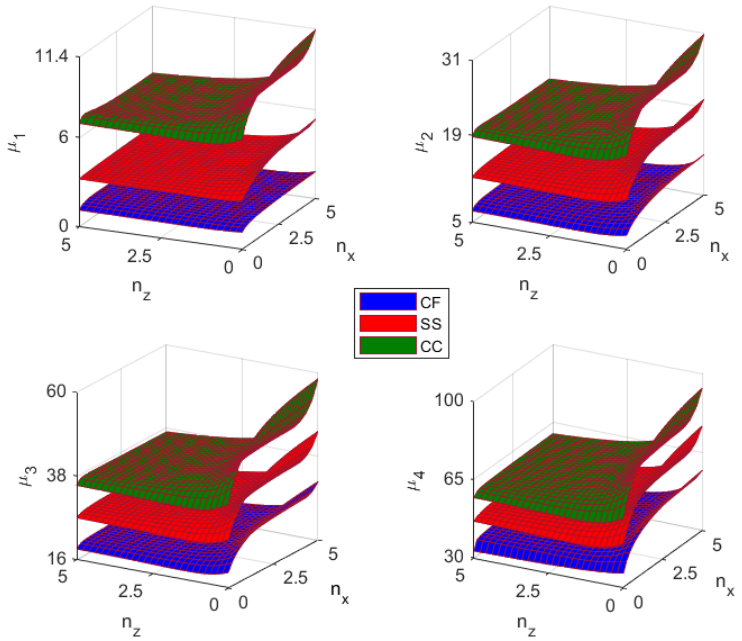


Figure 2. Variation of the first four frequency parameters with grading indices for various boundary conditions (*L*/*h*=20).

Figures 3, 4 and 5 illustrate the influence of the beam's slenderness ratio on the fundamental frequency parameter under various values of the grading indices for the S-S, C-C, C-F beam, respectively. An increase in the slenderness ratio results in a higher fundamental frequency parameter, independent of the grading indices and the boundary conditions. The figures clearly demonstrate the opposing effects of the $n_x$ and $n_z$ indices on frequency parameter, an increase in $n_z$ leads to a decrease in the frequency parameter (as seen from figures 3a, 4a, 5a), while an increase in $n_x$ results in increasing frequency parameter (as observed in figures 3b, 4b, 5b). Figures 3, 4 and 5 also indicate that the influence of the slenderness ratio on the fundamental frequency parameter becomes more pronounced when $L/h$<20. For $L/h$>20, the fundamental frequency parameters approach constant values, corresponding to those of the Euler-Bernoulli beam. This indicates that the shear deformable theories should be applied to short beams in the free vibration analysis of the BFG beam, while for the slender beams, the classical beam theory yields acceptable results for the frequency parameters.

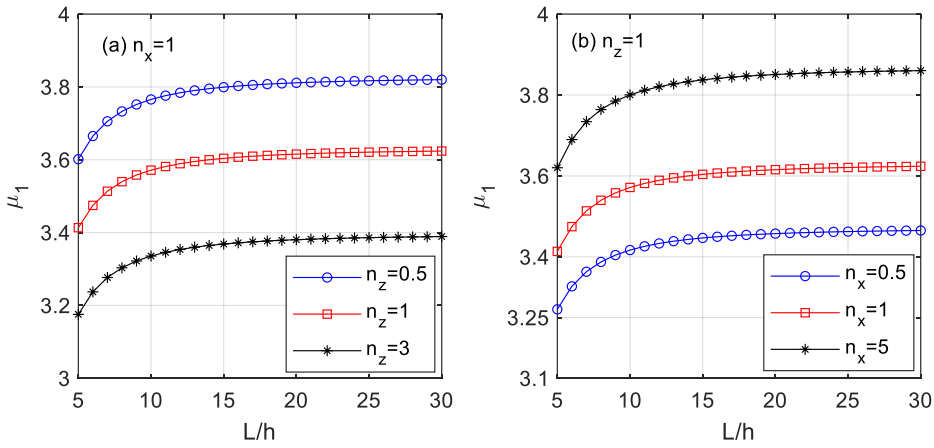


Figure 3. Variation of the frequency parameter $\mu_1$ of S-S BFG beam with slenderness ratio for different grading indices.

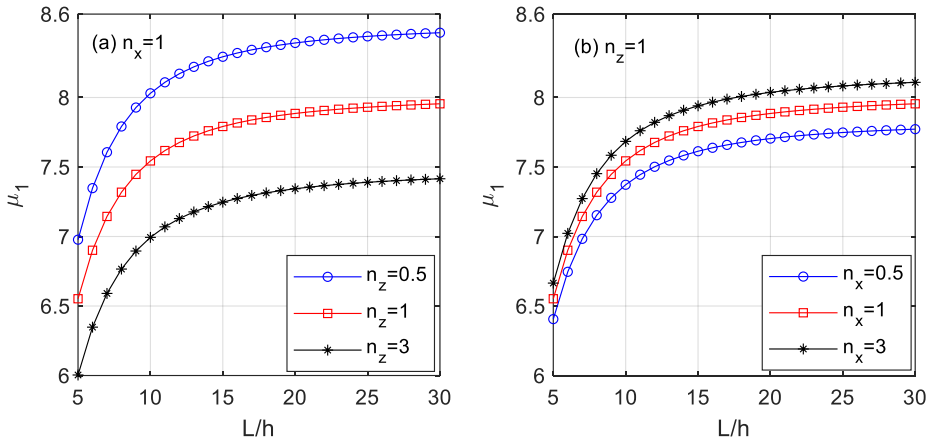


Figure 4. Variation of the frequency parameter $\mu_1$ of C-C BFG beam with slenderness ratio for different grading indices.

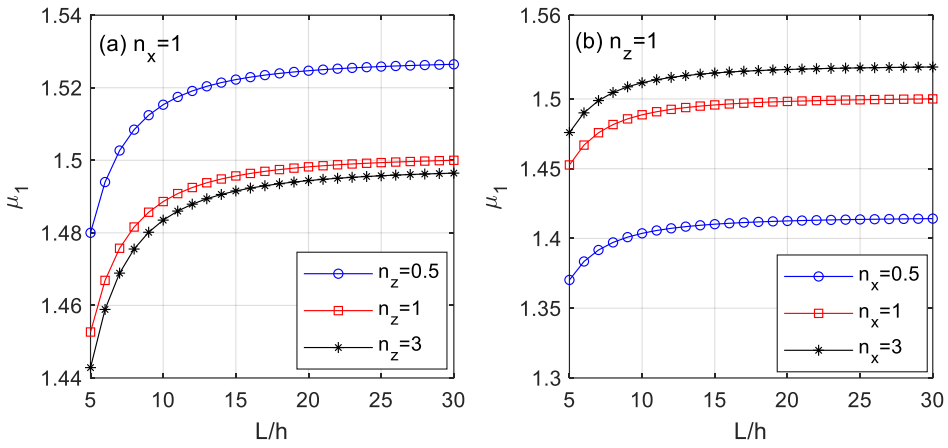


Figure 5. Variation of the frequency parameter $\mu_1$ of C-F BFG beam with slenderness ratio for different grading indices.

## 4. CONCLUSION

A trigonometric enriched beam element has been employed in this paper to investigate the free vibration of a four-phase BFG beam. The beam consists of four constituent materials whose properties vary continuously along both the length and thickness directions by a power law distribution, and they are evaluated using the Voigt model. Using Hamilton's principle and the higher-order shear deformation beam theory, the differential equations of motion for the BFG beam are obtained. The element stiffness and mass matrices are formulated by enriching the standard Lagrange and Hermite interpolations with trigonometric functions. The natural frequencies of four-phase BFG beams with different boundary conditions have been computed through numerical studies. The effects of grading indices, slenderness ratio and boundary conditions on the beam's natural frequency have been investigated. The main results obtained from the numerical analysis are summarized as follows:

- The proposed enriched beam element in this work proves to be effictive for modeling vibration behavior of four-phase BFG beam. Using the enriched element can obtain accurate frequency with only a small number of elements.
- Regardless of the boundary conditions, an increase in the index $n_x$ leads to higher frequency parameters, whereas increasing $n_z$ results in a decrease in the frequency parameters.
- An increase in the slenderness ratio lead to a higher fundamental frequency parameter, irrespective of the grading indices and boundary conditions.
- Under the considered boundary conditions, the C-C beam has the highest frequency parameter, whereas the frequency parameter calculated from C-F beam is the lowest.

## ACKNOWLEDGMENT

This research is funded by University of Transport and Communications (UTC) under grant number T2025-CB-010.

## REFERENCES

[1]. S. A. Sina, H. M. Navazi, H. Haddadpour, An analytical method for free vibration analysis of functionally graded beams, Materials & Design, 30 (2009) 741-747. https://doi.org/10.1016/j.matdes.2008.05.015

[2]. X. Wang, S. Li, Free vibration analysis of functionally graded material beams based on Levinson beam theory, Applied Mathematics and Mechanics, 37 (2016) 861-878. https://doi.org/10.1007/s10483-016-2094-9

[3]. V. Kahya, M. Turan, Finite element model for vibration and buckling of functionally graded beams based on the first-order shear deformation theory, Composites Part B: Engineering, 109 (2017) 108-115. https://doi.org/10.1016/j.compositesb.2016.10.039

[4]. M. Avcar, W. K. M. Mohammed, Free vibration of functionally graded beams resting on Winkler-Pasternak foundation, Arabian Journal of Geosciences, 11 (2018) 232. https://doi.org/10.1007/s12517-018-3579-2

[5]. I. Katili, T. Syahril, A. M. Katili, Static and free vibration analysis of FGM beam based on unified and integrated of Timoshenko's theory, Composite Structures, 242 (2020) 112130. https://doi.org/10.1016/j.compstruct.2020.112130

[6]. M. Şimşek, Bi-directional functionally graded materials (BDFGMs) for free and forced vibration of Timoshenko beams with various boundary conditions, Composite Structures, 133 (2015) 968-978. https://doi.org/10.1016/j.compstruct.2015.08.021

[7]. T. A. Huynh, X. Q. Lieu, J. Lee, NURBS-based modeling of bidirectional functionally graded Timoshenko beams for free vibration problem, Composite Structures, 160 (2017) 1178-1190. https://doi.org/10.1016/j.compstruct.2016.10.076

[8]. D. K. Nguyen, T. T. Tran, Free vibration of tapered BFGM beams using an efficient shear deformable finite element model, Steel and Composite Structures, 29 (2018) 363-377. https://doi.org/10.12989/scs.2018.29.3.363

[9]. Vu Thi An Ninh, Fundamental frequencies of bidirectional functionally graded sandwich beams partially supported by foundation using different beam theories, Transport and Communications Science Journal, 72 (2021) 362-377. https://doi.org/10.47869/tcsj.72.4.5

[10]. D. K. Nguyen, Q. H. Nguyen, T. T. Tran, V. T. Bui, Vibration of bi-dimensional functionally graded Timoshenko beams excited by a moving load, Acta Mechanica, 228 (2017) 141-155. https://doi.org/10.1007/s00707-016-1705-3

[11]. P. Ribeiro, Hierarchical finite element analyses of geometrically non-linear vibration of beams and plane frames, Journal of Sound and Vibration, 246 (2001) 225-244. https://doi.org/10.1006/jsvi.2001.3634

[12]. H. Y. Shang, R. D. Machado, J. E. Abdalla Filho, Dynamic analysis of Euler–Bernoulli beam problems using the generalized finite element method, Computers & Structures, 173 (2016) 109-122. https://doi.org/10.1016/j.compstruc.2016.05.019

[13]. Y. S. Hsu, Enriched finite element methods for Timoshenko beam free vibration analysis, Applied Mathematical Modelling, 40 (2016) 7012-7033. https://doi.org/10.1016/j.apm.2016.02.042

[14]. C. I. Le, N. A. T. Le, D. K. Nguyen, Free vibration and buckling of bidirectional functionally graded sandwich beams using an enriched third-order shear deformation beam element, Composite Structures, 261 (2021), 113309. https://doi.org/10.1016/j.compstruct.2020.113309

[15]. H. T. Thai, S. E. Kim, A simple higher-order shear deformation theory for bending and free vibration analysis of functionally graded plates, Composite Structures, 96 (2013) 165-173. https://doi.org/10.1016/j.compstruct.2012.08.025

[16]. M. Géradin, D. J. Rixen, Mechanical vibrations: theory and application to structural dynamics. John Wiley & Sons (2015).